

Joint Multivariate and Functional Modeling for Plant Traits and Reflectances

Philip A. White^{1*}, Michael F. Christensen², Henry
Frye³, Alan E. Gelfand² and John A. Silander, Jr. ³

¹Department of Statistics, Brigham Young University, Provo,
84602, Utah, USA.

²Department of Statistical Science, Duke University, Durham,
27708, Utah, USA.

³Department of Ecology and Evolutionary Biology, University of
Connecticut, Storrs, 06269, Connecticut, USA.

Contributing authors: pwhite@stat.byu.edu;
michael.f.christensen@duke.edu; henry.frye@uconn.edu ;
alan@duke.edu ; john.silander_jr@uconn.edu ;

Abstract

The investigation of leaf-level traits in response to varying environmental conditions has immense importance for understanding plant ecology. Remote sensing technology enables measurement of the reflectance of plants to make inferences about underlying traits along environmental gradients. While much focus has been placed on understanding how reflectance and traits are related at the leaf-level, the challenge of modelling the dependence of this relationship along environmental gradients has limited this line of inquiry. Here, we take up the problem of jointly modeling traits and reflectance given environment. Our objective is to assess not only response to environmental regressors but also dependence between trait levels and the reflectance spectrum in the context of this regression. This leads to joint modeling of a response vector of traits with reflectance arising as a functional response over the wavelength spectrum. To conduct this investigation, we employ a dataset from a global biodiversity hotspot, the Greater Cape Floristic Region in South Africa.

Keywords: conditional model validation; dimension reduction; functional data; Gaussian process convolution; Markov chain Monte Carlo; multivariate data

1 Introduction

Terrestrial ecosystems are reliant on the diversity and composition of plant species present in a community (O'Connor et al., 2017). Each species is comprised of a unique set of traits; these phenotypic characteristics include leaf size and shape, photosynthetic function, water content of leaves, and nutrient levels in leaves. The study of plant traits can provide insight into organismal function, plant–environment interactions, species coexistence and community dynamics, ecosystem structure and function, and biogeography and diversification. Thus, information on the diversity and abundance of plant traits can help us understand and predict complex ecological processes and responses to global change (Reich et al., 1997; Díaz and Cabido, 2001; Cadotte et al., 2011). Ecologists are particularly interested in how plant traits vary along spatial–environmental gradients since this can yield insights into the underlying principles of how communities originate and the convergence of survival strategies that plants evolved in response to their environment (Reich et al., 1999; McGill et al., 2006). These relationships provide a way to infer how ecosystems may change under novel environments, an important need as the rate human-driven environmental change increases (Schleuning et al., 2020).

Remote sensing provides an efficient and powerful way to measure plant traits and diversity at regional extents (Turner, 2014; Cavender-Bares et al., 2022). Image spectroscopy, which measures reflectance at high wavelength resolution across the reflectance spectrum, has been a prominent tool in predicting plant traits from remotely sensed imagery (Asner et al., 2011; Singh et al., 2015; Shiklomanov et al., 2016; Yang et al., 2016). At the leaf level, various wavelengths can be useful in predicting a suite of chemical, structural, and physiological traits (see Jacquemoud and Ustin, 2019a, and references therein) and the diversity of leaf-level reflectance within a community has been shown to be correlated with community plant diversity (Schweiger et al., 2018; Frye et al., 2021). Further, leaf-level spectra provide the basis for understanding mechanisms occurring at larger scales observed by remote sensing instruments flown aerially and in space.

There are still many gaps in our understanding of the relationship between plant optical properties and traits (Schimel et al., 2015; Jetz et al., 2016). One of these gaps is an explicit understanding of how traits and reflectance respond in tandem to environmental conditions. Because the relationship between reflectance and traits is an important crux of modern remote sensing efforts, their dependency over different environments is a major question to be explored. However, the high dimensionality of spectral data alongside the co-correlation of individual wavelengths and leaf traits poses a methodological hurdle. We offer novel joint modeling of traits and reflectances given environmental/habitat features. We consider joint modeling of two data types: multivariate continuous traits and functional reflectance data obtained at high wavelength resolution. We focus on understanding the effects of environmental regressors on plant traits and the reflectance spectrum at leaf-level, as well

as the relationships between traits and reflectance, captured through correlations, under this regression. Modeling such relationships requires a multivariate and functional response to regressors, as well as a model that relates these responses. Traits may, in fact, be ordinal or categorical, e.g., the degree or state of leaf pubescence or waxiness, but consideration of such traits is beyond our scope here.

Conceptually, we can build trait/reflectance models over different taxonomic scales, e.g., family, genus, species. Here, we work at family scale to obtain the largest sample size of trait/reflectance data. This is needed in order to best understand the very large number of correlations of interest, i.e., four traits by 500 wavelength bands, across $O(10^2)$ sites, each with individual environmental features. Thus, replicates are simply all of the observations available for the family in our database.

We remark that joint modeling of families, e.g., family level random effects, is not suitable because this implies a “global centering” of the families and borrowing strength across families. Exploratory analysis below suggests that, in our context, trait behavior across families is sufficiently different so that such shrinkage is not appropriate and that global parameters over families are not meaningful. Furthermore, different families have very different numbers of genera and species, further complicating joint interpretation. While analysis at a higher taxonomic scale is not appropriate with our data, our approach is applicable at higher scale and would enable potentially richer dependence stories.

We acknowledge that spatial dependence across sites is anticipated in joint modeling (White et al., 2022), where, with different intentions, White et al. (2022) focused on a marginal functional data model in a spatial setting. However, in attempting to obtain the needed large sample sizes for each of the families, we span regions that are disjoint and too spatially distant to employ sensible spatial modeling specifications. So, the observations are assumed to be conditionally independent. A fully spatial version, applied to an appropriate region, is a goal of future work.

Our primary contribution is jointly modeling a trait vector, \mathbf{T} , and a functional reflectance spectrum, \mathbf{R} , given environment/habitat features, \mathbf{E} . Specifically, our model uses a joint multivariate and function-on-scalar regression, after which we can extract the residual association between \mathbf{T} and \mathbf{R} given \mathbf{E} . We prefer a joint specification in the form $[\mathbf{T}, \mathbf{R} | \mathbf{E}]$ to conditional times marginal specification, $[\mathbf{T} | \mathbf{R}, \mathbf{E}] [\mathbf{R} | \mathbf{E}]$ since the former directly reveals how we capture association in the residuals between traits and reflectances at the replicate level. Specifically, we directly model the correlation between \mathbf{R} and \mathbf{T} through a joint model for the coefficients of functional bases and trait residuals. Our model also provides functional heterogeneity and heteroscedasticity.

Turning to model assessment, under our specifications, we are assuming dependence among the traits, dependence across the reflectance spectrum, and dependence between traits and reflectances. So, model comparison should be based upon conditional prediction. We demonstrate improved out-of-sample

prediction under the dependence model vs. an independence model given partial information at a site, i.e., when predicting traits or reflectances which we didn't collect at the site.

Multivariate modeling in ecology is well established (see, e.g., [Schliep and Hoeting, 2013](#); [Clark et al., 2017](#)). In particular, modeling the joint patterns of plant traits improves prediction (see [Schliep et al., 2018](#)). Functional data analysis (FDA) is widely used to represent curves with continuous domains (see [Ramsay, 2005](#); [Ramsay and Silverman, 2007](#), for pioneering work in the field). In general, FDA relies on representing the function through a low-rank representation (e.g., splines, wavelets, or kernels). Our challenge is relating multivariate data response specifications for traits to functional data response specifications for reflectance to allow relational inference between the responses.

We use our modelling framework to elaborate upon the joint **T**, **R**, and **E** relationships for four families within the Greater Cape Floristic Region (GCFR) of South Africa. The GCFR is of special importance to global biodiversity as it contains two adjacent global biodiversity hotspots, the Fynbos and Succulent Karoo biomes. Such biodiversity hotspots are important to global biodiversity conservation because they are regions that not only contain large numbers of species, but also have many species that are not found anywhere else on Earth ([Myers et al., 2000](#); [Latimer et al., 2005](#); [Born et al., 2006](#)). The four families we focus our analysis on- the Aizoaceae, Asteraceae, Proteaceae, and Restionaceae- are iconic families found throughout the GCFR and are comprised of large species radiations ([Manning and Goldblatt, 2012](#); [Manning, 2013](#)). We focus on four leaf traits- leaf water content, leaf mass per area, percent nitrogen, and succulence (water content/leaf area)- as these are both commonly used traits in the trait ecology and remote sensing literature and represent major evolutionary strategies among plants (see [Wright et al., 2004](#); [Jacquemoud and Ustin, 2019b](#), and references therein).

We continue the paper with a presentation of the dataset and exploratory data analysis that motivates our analysis in Section 2. Based on data characteristics demonstrated in our exploratory data analysis, we present a joint model for multivariate traits and functional reflectance data in 3. We then offer interpretation of our results for each of the four families in Section 4 and conclude with a brief summary and potential future work.

2 The Dataset

We model plant trait and reflectance data at the family level, fitting each of the families Aizoaceae, Asteraceae, Proteaceae, and Restionaceae individually. These four families are generally speciose in the Greater Cape Floristic Region (GCFR) in South Africa, though the Proteaceae and Restionaceae have less prevalence in the arid regions of the GCFR ([Manning and Goldblatt, 2012](#); [Manning, 2013](#)). In Table 1, we provide the number of times each family is observed in the dataset as well as the number of genera and species within each

family. We see that the families differ dramatically in how often they appear, as well as how many genera and species appear for that family. Although some plant families have similar spatial ranges, they are not generally co-located (See Figure 1).

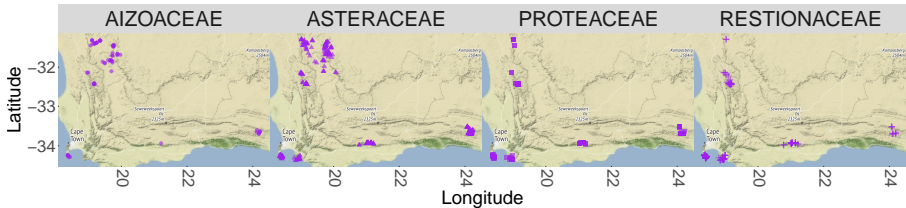


Fig. 1 Locations of trait and reflectance data for each plant family.

Table 1 Number of observations and genera for each family considered in this study.

Family	Observations (N)	Genera	Species
Aizoaceae	64	17	45
Asteraceae	310	58	197
Proteaceae	110	10	58
Restionaceae	152	16	89

We analyze four continuous leaf traits – leaf water content (LWC), leaf mass per area (LMA), percent Nitrogen (pN), and leaf succulence (LS) along with leaf reflectance as a function over wavelength $w \in [450, 950]$ nanometers, observed as a 500 dimensional reflectance vector, by nanometer. Leaf reflectance was measured from sun leaves collected from the top of the canopy using a USB-4000 Spectrometer (Ocean Optics, Largo, Florida, USA) with a leaf clip attachment. For further details on spectra and trait data collection see [Frye et al. \(2021\)](#) and [Aiello-Lammens et al. \(2017\)](#), respectively. In some cases, at a site, for a given species within a family, we have more than one trait observation and/or reflectance observation. Again, viewing the sites as replicates, such observations are averaged to obtain a single \mathbf{T} value and a single \mathbf{R} value for the site. However, there may be duplication of replicates at a site because more than one species is sampled at many sites.

We analyze traits and and reflectance on the log-scale as a standard transformation that improves the assumptions of our Gaussian model (discussed in Section 3 below). We define the response as $\mathbf{y}_j = (\mathbf{T}'_j, R_j(w))'$, where \mathbf{T}_j is a vector of four plant traits (on the log scale) and $R_j(w)$ is a log-reflectance function. We model $R_j(w)$ as a random function where, again, $R_j(w)$ is observed at 500 wavelengths at one nanometer (nm) spacing between 450-949 nm. For both traits and reflectance, we use j to index replication within family.

To visualize the overall patterns present in the data, we plot all log reflectances by family in Figure 2, including the family-specific mean. All families show some similarities with relatively low reflectance for blue (450 - 500

6 *Joint Modeling of Plants Traits and Reflectance*

nm) and some red wavelengths (600 - 675 nm), with a local maximum around 550 nm (green). Reflectance increases in the red (around 700 nm) and remains uniformly high in the near-infrared (740-949 nm). In Figure 2, we also include box plots of the observed log plant traits for each family. Although traits and reflectances are similar across families, each family shows different amounts of heterogeneity.

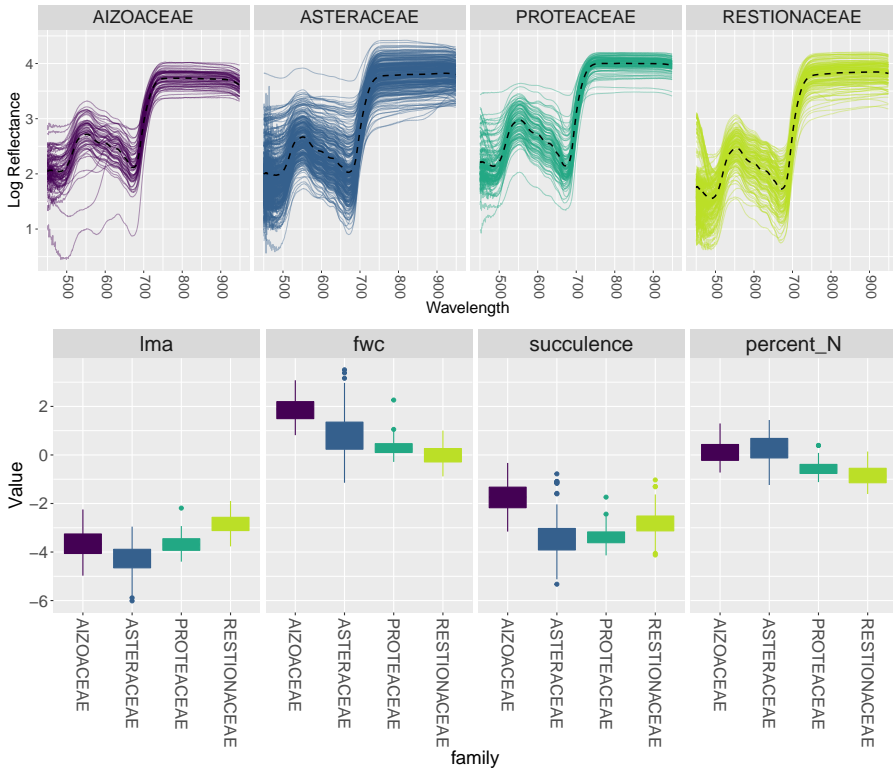


Fig. 2 (Top) All reflectance curves for each family. Dashed line represents the family-specific mean. (Bottom) Boxplots for the four plant traits, paneled by each family.

To jointly explain plant traits and reflectance, we use four environmental covariates in \mathbf{E}_j : (i) elevation (Elevation30m), (ii) annual precipitation (Gmap), (iii) rainfall concentration (RFL.CONC), and (iv) minimum average temperature in January, the peak of the austral summer (tminave 01c). Elevation data was derived from 30 m resolution digital elevation maps (JPL, 2020) while the other climate variables were taken from Schulze (1997). We also introduce the family-level plant abundance at the site of the j th replicate as an explanatory variable. Though not a customary environmental predictor, we include it in \mathbf{E}_j to play the role of a proxy for site level environmental suitability for the family. That is, the other environmental regressors above operate at larger spatial scales and we seek to supply a more local regressor.

As a measure of suitability, we define abundance for a family at a site as the aggregated percent cover of all species in that family at the site. Due to some misalignment between the sites in this analysis and sites with available percent cover, we estimate percent cover using ordinary kriging on the scale of $\log(x+1)$ to yield predictions on $[0, \infty)$ as well as to deal with many zeros. Specifically, we use an exponential covariance function with parameters estimated from empirical semivariograms.

To motivate our analysis, we calculate the empirical correlation between the environmental variables and each log trait and log reflectance for each family. We plot these correlations in Figure 3. Apart from a few exceptions,

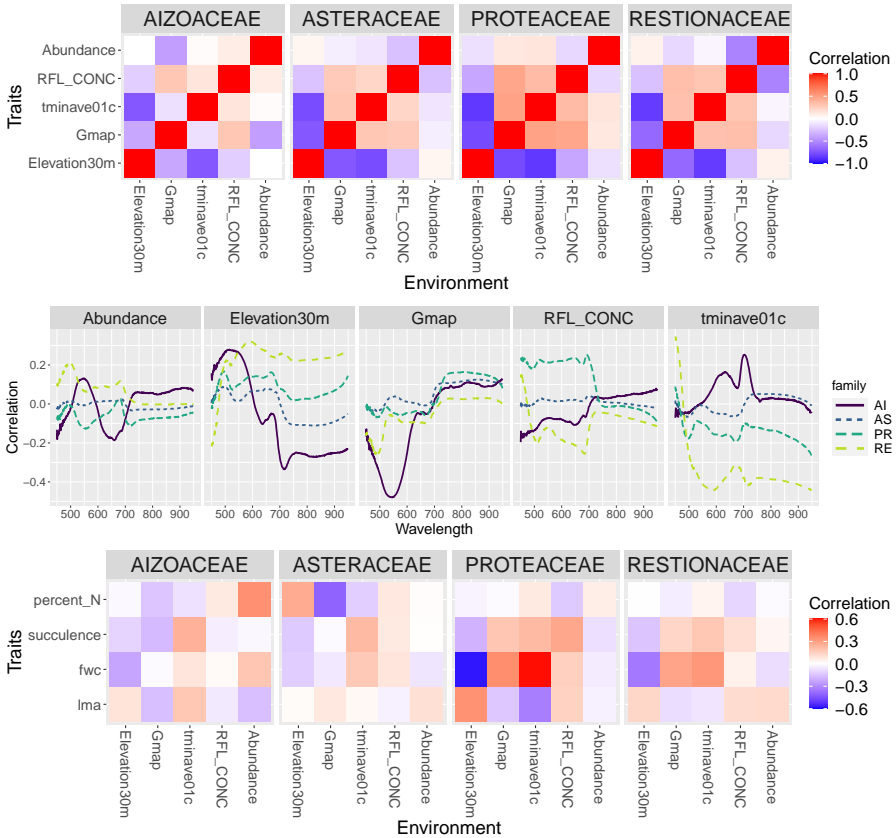


Fig. 3 Empirical correlations between environmental predictors (Top) Themselves, (Middle) log traits, and (Bottom) log reflectance. The results are presented for each plant family. The labels “AI”, “AS”, “P”, and “R” represent Aizoaceae, Asteraceae, Proteaceae, and Restionaceae, respectively.

most correlations between \mathbf{E}_j and \mathbf{T}_j are weak, not surprising given only modest correlations between traits and environment within the region (Mitchell et al., 2015; Aiello-Lammens et al., 2017) and at global and other local scales

(Wright et al., 2004; Wright and Sutton-Grier, 2012). Importantly, there is very little common correlation pattern shared across families, expected given the large differences in growth form and likely ecological strategies that each lineage has evolved. As with traits, examining the empirical correlations between the environmental variables and the log reflectance curves reveals little common pattern between the families. However, importantly, there are evident differences in the correlations between reflectance and environment over the wavelength spectrum, suggesting the need for wavelength-varying coefficients in functional modeling of reflectance as a response.

We present the empirical correlations between log traits and log reflectance in Figure 4. There are few similarities in the trait-reflectance correlations

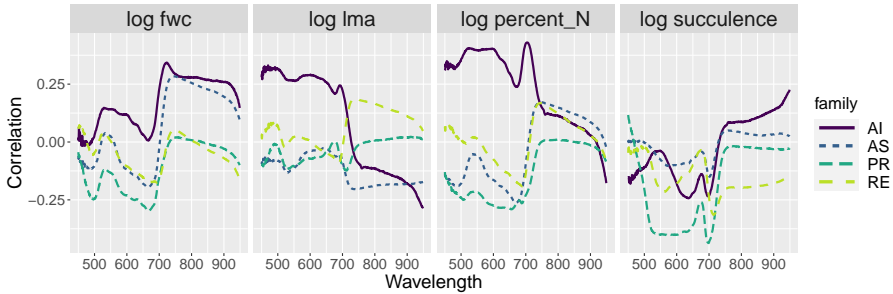


Fig. 4 Empirical correlations between traits and log reflectances for each family. The labels “AI”, “AS”, “P”, and “R” represent Aizoaceae, Asteraceae, Proteaceae, and Restionaceae, respectively.

among the families. In general, the families with more data have weaker correlations between traits and reflectances. Families with more genera and species likely represent speciation “hot-beds”, e.g., see Verboom et al. (2009), Pirie et al. (2016), and Mitchell et al. (2017), where we would expect that the number of species would result in greater variability of traits and reflectance within lineages. It has been shown that higher within-group trait variation dilutes trait associations (Laughlin et al., 2017; Andregg et al., 2018) and thus we may anticipate a similar effect for trait and reflectance relationships. Again, our goal is to assess the strength of these trait/reflectance relationships while accounting for environment.

Our exploratory analysis shows that the relationships between traits, reflectance, and environmental predictors (See Figures 3 and 4) differ greatly across families, both in shape and magnitude. Further, in preliminary modeling efforts, we found no benefit to modeling the families jointly. Therefore, as noted above, we model each family separately.

3 Model and Methods

3.1 The joint specification

Since we model the families individually, we need only subscript the replicates within a family. So, consider vector \mathbf{T}_j , an $s \times 1$ vector of trait responses for replicate j . We assume, after the log-transformation, that this vector can be modeled to follow a multivariate normal distribution. With a binary or categorical response we would view the corresponding entry in \mathbf{T}_j as *latent*, driving the observed response. We model \mathbf{T}_j as

$$\mathbf{T}_j = \boldsymbol{\alpha}^{(T)} + \mathbf{B}^{(T)}\mathbf{E}_j + \mathbf{U}_j^{(T)}. \quad (1)$$

Here, $\boldsymbol{\alpha}^{(T)}$ are trait-specific intercepts, \mathbf{E}_j is a vector of environmental predictors, say $p \times 1$, for replicate j and $\mathbf{B}^{(T)}$ is a $s \times p$ matrix of trait-specific regression coefficients. The $\mathbf{U}_j^{(T)}$ are pure errors, i.i.d. $\sim MVN(\mathbf{0}, \Omega^{(T)})$.

We model the reflectance as a functional response variable, observed at 500 wavelengths, with wavelengths denoted by w 's. Specifically,

$$R_j(w) = \alpha^{(R)}(w) + \mathbf{E}'_j\boldsymbol{\beta}^{(R)}(w) + \mathbf{K}'_U(w)\mathbf{U}_j^{(R)} + \psi_j(w). \quad (2)$$

Here, $\alpha^{(R)}(w) = \mathbf{K}'_\alpha(w)\boldsymbol{\alpha}^{*(R)}$ is a wave-length varying intercept, where dimension reduction is given through l basis functions in $\mathbf{K}'_\alpha(w)$. \mathbf{E}_j is, as above with the $p \times 1$ wavelength specific coefficient vector $\boldsymbol{\beta}^{(R)}(w) \equiv \mathbf{B}^{(R)}\mathbf{K}_\beta(w)$. That is, we imagine $\mathbf{K}_\beta(w)$ as an $m \times 1$ vector of basis functions or convolution functions with $\mathbf{B}^{(R)}$ an $p \times m$ matrix of coefficients providing dimension reduction. Aggregating, $\boldsymbol{\beta}_{p \times 500}^{(R)} = \mathbf{B}^{(R)}\mathbf{K}'_\beta$ where \mathbf{K}_β is $500 \times m$.

Further, again using dimension reduction, the term $\mathbf{K}'_U(w)\mathbf{U}_j^{(R)}$ introduces the $q \times 1$ replicate level vector $\mathbf{U}_j^{(R)}$ of reflectance random effects to supplement the fixed effects contribution. These random effects vectors adopt $q \ll 500$ to provide a dimension reduction for the reflectances. More will be said about the choice of q below. The $\mathbf{K}_U(w)$ can be collected into a $500 \times q$ matrix, \mathbf{K}_U . Finally, the $\psi_j(w)$ provide independent wavelength specific pure error terms with variances $\sigma^2(w)$. We model $\log(\sigma^2(w)) = \mathbf{K}_\sigma\boldsymbol{\gamma}_\sigma$ as a linear spline as in [White et al. \(2022\)](#). The entire reflectance response vector for replicate j becomes $\mathbf{R}_j = \boldsymbol{\alpha}^{(R)} + \mathbf{K}_\beta^T\mathbf{B}^{(R)'}\mathbf{E}_j + \mathbf{K}_U\mathbf{U}_j^{(R)} + \boldsymbol{\Psi}_j$.

We introduce dependence between the traits and reflectances, the T 's and the R 's, through the U 's. That is, the dependence is at the replicate level.

Specifically, we assume $\begin{pmatrix} \mathbf{U}_j^{(T)} \\ \mathbf{U}_j^{(R)} \end{pmatrix}$ is distributed as a mean $\mathbf{0}$ multivariate normal with covariance matrix $\boldsymbol{\Omega} = \begin{pmatrix} \boldsymbol{\Omega}^{(T)} & \boldsymbol{\Omega}^{(TR)} \\ \boldsymbol{\Omega}^{(TR)'} & \boldsymbol{\Omega}^{(R)} \end{pmatrix}$. As a result the induced

covariance matrix for $\begin{pmatrix} \mathbf{T}_j \\ \mathbf{R}_j \end{pmatrix}$ becomes $\Sigma = \begin{pmatrix} \mathbf{\Omega}^{(T)} & \mathbf{\Omega}^{(TR)}\mathbf{K}'_U \\ \mathbf{K}_U\mathbf{\Omega}^{(TR)'} & \mathbf{K}_U\mathbf{\Omega}^{(R)}\mathbf{K}'_U + \mathbf{D}_\psi \end{pmatrix}$

where \mathbf{D}_ψ is the diagonal matrix of pure error reflectance variances. From this matrix we can extract all covariances and correlations. If $\mathbf{\Omega}^{(TR)}$ is a matrix of zeros, then we have an independence model, which we denote as $[\mathbf{T}|\mathbf{E}][\mathbf{R}|\mathbf{E}]$.

We provide details of the dimension reduction used in Section 3.2, justify the use of the joint model through cross validation in Section 3.4 and Appendix B, and then present the results using the joint model in Section 4.

3.2 Dimension reduction details

Following White et al. (2022), we specify the low-rank functional terms wavelength-varying intercept $\alpha^{(R)}(w)$, random effects $\mathbf{K}'_U(w)\mathbf{U}_j^{(R)}$, and $\beta^{(R)}(w)$ through process convolutions enabling simple connection to Gaussian processes (GPs). That is, the kernels of the process convolution connect the low-rank process to the GP covariance (Higdon, 2002). For every basis, we include an intercept so that the wavelength-varying intercepts, regression coefficients, and variances have an overall centering.

We use a rich specification for the wavelength-varying intercept $\alpha^{(R)}(w)$, employing Gaussian kernels with wavelength knots spaced every 10 nm from 450-950 nm ($N_\alpha = 52$, in total, including the intercept) to obtain $\mathbf{K}_\alpha(w)$. To specify the wavelength-varying random effects through $\mathbf{K}_U(w)$, we use Gaussian kernels with wavelength knots spaced every 25 nm from 450-950 nm ($N_U = 22$, in total, including an intercept). To specify wavelength-varying coefficient functions, we use Gaussian kernels with wavelength knots spaced every 100 nm from 450-950 nm ($N_\beta = 7$, including the intercept) for $\mathbf{K}_\beta(w)$. We allow the scale parameters for the dimension-reduced coefficient to be unknown. However, we fix the bandwidth of the Gaussian kernels to be 1.5 times the kernel spacing to alleviate well-known lack of identifiability with scale and range parameters of Gaussian process models (see, e.g., Zhang, 2004). Lastly, we use a linear splines with interior knots every 50 nm from 475-925 nm to specify \mathbf{K}_σ ($N_\sigma = 12$, in total). The selection of knot spacing chosen here is motivated by a sensitivity analysis in White et al. (2022), where the simplest model is chosen that does not significantly decrease model performance.

3.3 Prior Distributions, Model Fitting, and Prediction

We adopt weakly informative prior distributions for all trait regression coefficients and the intercepts of the wavelength-varying parameters for reflectance. However, for wavelength-varying intercept and regression coefficient functions, we have unknown scale parameters that shrink the low-dimensional functional bases toward zero. Overall, these priors assume that the wavelength-varying parameters receive an overall centering given by associated intercepts. We use proper prior distribution with large variance for all variance and covariance parameters. Specifically, we use the following prior distributions:

$$\begin{aligned}
\boldsymbol{\alpha}_1^{*(R)} &\sim N(0, 10^3), & \gamma_{\sigma_1} &\sim N(0, 10^4) \\
\boldsymbol{\alpha}_j^{*(R)} &\stackrel{iid}{\sim} N(0, \sigma_\alpha^2); j = 2, \dots, N_\alpha, & \gamma_{\sigma_j} &\stackrel{iid}{\sim} N(0, 9); j = 2, \dots, N_\sigma, \\
\mathbf{B}_{k1}^{(R)} &\stackrel{iid}{\sim} N(0, 10^3); k = 1, \dots, p, & \boldsymbol{\Omega}^{-1} &\sim \text{Wishart}(s + N_U + 1, 10^{-3}\mathbb{I}), \\
\mathbf{B}_{kj}^{(R)} &\stackrel{iid}{\sim} N(0, \sigma_\beta^2); k = 1, \dots, p; j = 2, \dots, N_\beta, & \sigma_\alpha^{-2} &\sim \text{Gamma}(1, 1), \\
\boldsymbol{\alpha}_k^{(T)} &\stackrel{iid}{\sim} N(0, 10^3); k = 1, \dots, p, & \sigma_{\beta_k}^{-2} &\stackrel{iid}{\sim} \text{Gamma}(1, 1); k = 1, \dots, p, \\
\mathbf{B}_{jk}^{(T)} &\stackrel{iid}{\sim} N(0, 10^3); j = 1, \dots, s; k = 1, \dots, p, & &
\end{aligned} \tag{3}$$

Letting $\boldsymbol{\eta}$ denote all model parameters, we estimate $\boldsymbol{\eta}$ using Markov chain Monte Carlo (MCMC). So, our model fitting yields M samples from the posterior distribution of all model parameters $\boldsymbol{\eta}_1, \dots, \boldsymbol{\eta}_M$. For all parameters except γ_σ , we are able to use a Gibbs sampler because posterior conditional distributions can be found in closed form. For γ_σ , we use a Metropolis within Gibbs update with a Gaussian random walk proposal distribution. We run this algorithm for 200,000 iterations, discard a burn-in period of 100,000 iterations, and, to limit memory requirements, thin the remaining 100,000 samples to 5,000 samples. During the burn-in period of the model-fitting, we tune acceptance rate to be between 0.2 and 0.6 during the burn-in period of the model fitting. Specific details of the posterior conditional distributions are provided in Appendix A.

Beyond the primary goal of inferring relationships between environment, traits, and reflectance, a further use for this model is prediction of traits or reflectance in the frequent scenario where, at a given site, measurements of either plant traits or reflectances were made but not both. In such settings, the residuals/random effects U would be attached to only partially observed samples. Therefore, predictions for reflectance or traits are made by conditionally predicting U , $U^{(R)}|U^{(T)}$ or $U^{(T)}|U^{(R)}$, respectively. Under our model, these predictions rely on conditional normal theory. To illustrate this, we drop the j subscript and consider prediction using a single posterior sample $\boldsymbol{\eta}_m$ of all model parameters. The conditional prediction of traits or reflectance would, respectively, be

$$\begin{aligned}
\tilde{T}_m &= \boldsymbol{\alpha}_m^{(T)} + \mathbf{B}_m^{(T)} \mathbf{E} + \mathbf{U}_m^{(T)}, \\
\tilde{R}(w) &= \alpha_m^{(R)}(w) + \mathbf{E}' \boldsymbol{\beta}_m^{(R)}(w) + \mathbf{K}'_U(w) \mathbf{U}_m^{(R)} + \psi_m(w),
\end{aligned}$$

where $\mathbf{U}_m^{(T)} \sim N(\boldsymbol{\mu}_{T|R}, \boldsymbol{\Sigma}_{T|R})$, $\boldsymbol{\mu}_{T|R} = \boldsymbol{\Omega}^{(TR)} \boldsymbol{\Omega}^{(R)}^{-1} \mathbf{U}_m^{(R)}$, $\boldsymbol{\Sigma}_{T|R} = \boldsymbol{\Omega}^{(T)} - \boldsymbol{\Omega}^{(TR)} \boldsymbol{\Omega}^{(R)}^{-1} \boldsymbol{\Omega}^{(TR) \prime}$, $\mathbf{U}_m^{(R)} \sim N(\boldsymbol{\mu}_{R|T}, \boldsymbol{\Sigma}_{R|T})$, $\boldsymbol{\mu}_{R|T} = \boldsymbol{\Omega}^{(RR)} \boldsymbol{\Omega}^{(T)}^{-1} \mathbf{U}_m^{(T)}$, and $\boldsymbol{\Sigma}_{R|T} = \boldsymbol{\Omega}^{(R)} - \boldsymbol{\Omega}^{(TR) \prime} \boldsymbol{\Omega}^{(T)}^{-1} \boldsymbol{\Omega}^{(TR)}$. This process is repeated for all posterior samples $\boldsymbol{\eta}_1, \dots, \boldsymbol{\eta}_M$, yielding a set of M predictions.

3.4 Model Comparison

We justify the joint model specification $[T, R|E]$ by comparing conditional predictive performance using 10-fold cross-validation. Specifically, we compare the joint model to a model where traits and reflectance are independent $[T|E][R|E]$. For each fold of the cross validation, we hold out 10% of all traits (jointly), as well as 10% of reflectance spectra (the entire spectrum). The traits and reflectance spectrum are held out exactly one time in the 10-fold cross validation. We adopt this comparison approach to mirror the scenario above where either plant traits or reflectances are measured but not both. Of course, other holdout schemes could be investigated.

We focus our comparison here on the Asteraceae family because it has the most data to help in estimating the proposed correlation structure. The model comparison results are summarized in Table 2, while the comparison results for the other families are in Appendix B. We compare models by using predicted root mean squared error (RMSE), mean absolute error (MAE), and the mean energy score (ES),

$$ES(F, \mathbf{x}) = \frac{1}{2} \mathbb{E}_F \|\mathbf{X} - \mathbf{X}'\| - \mathbb{E}_F \|\mathbf{X} - \mathbf{x}\|,$$

where \mathbf{X}, \mathbf{X}' follow the same distribution F and \mathbf{x} is a vector of hold-out values (see [Gneiting and Raftery, 2007](#)). To estimate this empirically, from a set of posterior predictions $\mathbf{X}_1, \dots, \mathbf{X}_M$, forming \hat{F} for a vector \mathbf{x} , the energy score is calculated as

$$ES(\hat{F}, \mathbf{x}) = \frac{1}{2M^2} \sum_{m=1}^M \sum_{m'=1}^M \|\mathbf{X}_m - \mathbf{X}_{m'}\| - \frac{1}{M} \sum_{m=1}^M \|\mathbf{X}_m - \mathbf{x}\|,$$

and we average this for all hold-out vectors. The ES compares multivariate predictions to multivariate quantities and is a proper scoring rule ([Gneiting and Raftery, 2007](#)). We use the ES as our primary model selection criterion when predicting all traits or all reflectances. We present MAE and RMSE for each trait individually but, for simplicity, choose to average these quantities for reflectances over all wavelengths. On the other hand, because either traits or reflectances are predicted jointly conditioning on the other, a single mean ES is given for all traits and for all reflectances, respectively.

For the Asteraceae family, the joint model improves out-of-sample prediction performance for reflectances and all traits. Overall, the benefit of the joint model is much larger for reflectance than traits, and this benefit is substantial. Based on these findings, we use the joint model to present interpretation of the results.

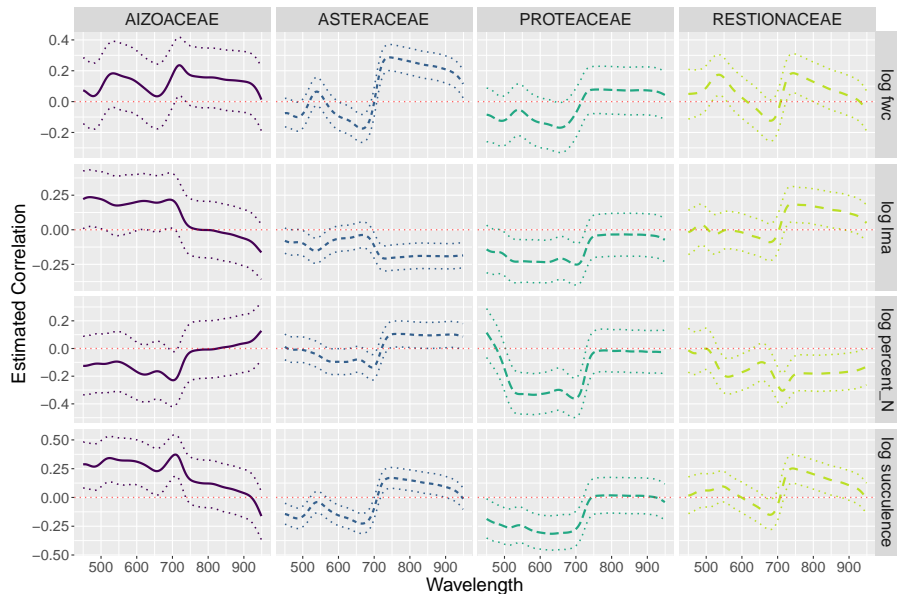
Table 2 Model comparison between joint and independent models for Asteraceae.

Quantity	Model	MAE	RMSE	ES
log LMA	[T E][R E]	0.449	0.557	0.826
log FWC		0.646	0.814	
log LS		0.533	0.706	
log pN		0.395	0.495	
log Reflectance	[T E][R E]	0.543	0.981	16.396
log LMA	[T, R E]	0.398	0.517	0.658
log FWC		0.465	0.612	
log LS		0.401	0.546	
log pN		0.343	0.457	
log Reflectance	[T, R E]	0.166	0.244	3.703

4 Results

4.1 Correlation Between Traits and Reflectance

We focus our discussion on the estimated correlations between the plant traits (log leaf water content, log leaf mass area, log percent Nitrogen, and log succulence) and the log reflectances. In Figure 5, we plot the estimated correlations between log traits and reflectance for the Asteraceae, Proteaceae, and Restionaceae families. Specifically, we plot the posterior mean and 90% credible intervals for between trait and reflectance correlation.

**Fig. 5** The estimated correlation between reflectance and all plant traits provided through Ω .

Given the environmental variables, we observe relatively weak relationships (typically between 0.2 to -0.2) between traits and reflectance. This finding is not entirely unexpected (Laughlin et al., 2017; Pau et al., 2022; Wang et al., 2022), despite the amount of literature devoted to the strength of relationships and prediction potential between traits and reflectance within species and communities (see Jacquemoud and Ustin (2019b) for a review). Fewer studies such as ours examine how these relationships vary across species within broader lineages such as families. The fact that we observe differing \mathbf{T} and \mathbf{R} relationships between families aligns with our expectation that the species within these families are comprised of various suites of leaf traits that in turn represent different adaptive strategies and ancestral constraints. In other words, spectra represent underlying biology, a point underscored in recent literature (Meireles et al., 2020; Cavender-Bares et al., 2022; Kothari and Schweiger, 2022).

Further, we again highlight the fact that we are examining \mathbf{T} and \mathbf{R} relationships jointly given environment. This type of inquiry has often been done indirectly through controlled experimental manipulations (Thenot et al., 2002; Inoue and Peñuelas, 2006; Ripullone et al., 2011; Caturegli et al., 2020) or along environmental gradients (Coops et al., 2002; Asner et al., 2009). What our modelling shows is the explicit joint effects that environment has in terms of traits and reflectance. In cases of 0 or insignificant correlation we interpret that either the chosen environmental parameters have little effect on that lineage's traits (which in turn affect reflectance) or that the species within the lineage differ in their responses to the same environmental parameter resulting in low signal, i.e., the ecological fallacy. In the case of significant correlations, we observe shifts in \mathbf{T} and \mathbf{R} relationships that suggest lineage-wide signals indicative of ecological and evolutionary processes such as adaptation or ancestral constraints.

We observe relatively weak relationships between log reflectance and log leaf water content with one exception. For wavelengths greater than 700 nm (red and near-infrared [NIR]), we estimate that Asteraceae's reflectance is positively correlated with leaf water content. The near infrared portion of the spectrum is well known in several instances to be a signal for various forms of water content in leaves (Pu et al., 2003; Rodríguez-Pérez et al., 2007; Seelig et al., 2008) and canopies (Peñuelas et al., 1993; Penuelas et al., 1997). On the other hand, Aizoaceae, Proteaceae, and Restionaceae show no or few wavelengths where the 90% credible interval excludes 0. Note that this does not indicate that leaf water content and reflectance are unrelated in these lineages, but rather, after accounting for environment, these correlations are negligible. We suspect that the leaf water signal observed in the Asteraceae is attributable to the fact that the lineage has one of the broadest distributions extending from the arid Succulent Karoo to more mesic Fynbos.

For log leaf mass per area, we generally expected to observe the strongest correlation within the near-infrared region (NIR), i.e., wavelengths greater than 700 nm (Asner et al., 2011; Jacquemoud and Ustin, 2019c; Serbin et al., 2019). Within the NIR, some families exhibit positive correlations

with reflectance (Restionaceae), while others have negative correlations with reflectance (Asteraceae). Interestingly, Proteaceae has negative correlations for wavelengths between 500 and 725 nm for leaf mass per area. This could be the result of other co-correlated traits such as photosynthetic pigments that more often affect the visible region. There is some limited evidence within species for the negative correlation in the visible region for leaf mass per area (Oucival et al., 1999).

Nitrogen within leaves is typically linked to the visible region of the spectrum (450-700 nm) given its strong links to the pigment chlorophyll, though there are nitrogen signals found at longer wavelengths (Jacquemoud and Ustin, 2019d). For Aizoaceae and Asteraceae, the relationship between log pN and reflectance appears to be weak for all wavelengths, suggesting no lineage wide signals across the environmental range present in the study. Proteaceae shows negative correlations between log pN and reflectance for wavelengths between 500 and 725 nm. Although weak, the estimated relationship between pN and reflectance is negative for most wavelengths greater than 550 nm for Restionaceae.

Leaf succulence is calculated by dividing the leaf area by leaf water content such that succulence represents the amount of water distributed throughout the leaf. Thus, we expected results like that for leaf water content. Overall, our results matched these expectations, but the results did have different significance compared to water content. Except for the Restionaceae, the other families had significant relationships within the visible range (wavelengths below 700 nm) which was surprising given the typically stronger signal of water within near infrared range. However, previous studies have found relationships between water content and the visible range attributed to the link between plant water status and photosynthetic machinery (Thenot et al., 2002; Inoue and Peñuelas, 2006; Ripullone et al., 2011; Hmimina et al., 2014). The Aizoaceae, a lineage dominated by succulent plants, now displayed significant, albeit weak, positive correlations for wavelengths below 700 nm. Asteraceae has weak negative correlations between succulence and log reflectance for wavelengths less than 700 nm but weak positive correlations for wavelengths greater than 700 nm. Proteaceae shows negative correlations between succulence and log reflectance for wavelengths less than 725 nm, but the correlations are essentially 0 otherwise. As with LMA, succulence and reflectance have very weak relationships for Restionaceae.

4.2 Effects of the environmental and abundance predictors

We report the estimated effect of the environmental predictors and abundance on reflectance and traits. As discussed in Section 2, we have centered and scaled the covariates to aid in interpretation of the results. In Figure 6, we plot the four estimated coefficient functions and associated 90% credible intervals for each family. In Figure 7, we plot the 90% credible intervals for the regression coefficients for each trait. Again, abundance is unlike the other

environmental covariates in that it is not a direct driver of leaf traits and subsequent reflectances. It is viewed as a proxy for unmeasured local environmental contributing to the “success” of species based on their biomass.

In terms of interpretation, we re-emphasize the fact that these models treat traits and reflectance jointly. As shown in Figure 3, the reflectance spectra within each lineage have clear correlations with environmental parameters. Our results in Figure 6 are much weaker and less varied for all families, which was expected given the joint nature of the model where more variation is likely to be attributable to leaf traits (Laughlin et al., 2017; Pau et al., 2022; Wang et al., 2022). We interpret Figure 6 as capturing the signal of family-wide spectral responses to environment that are being driven by traits that are not currently measured, e.g., pigments, leaf surface features, or other measures of leaf anatomy. We would expect the trait and environment relationships in figure 7 to roughly match the initial correlations in Figure 3 given that it is traits that respond to environment and are subsequently manifested in the reflectance spectra. All covariate effects should be interpreted as the estimated effect of the particular environmental covariate holding all other environmental covariates constant.

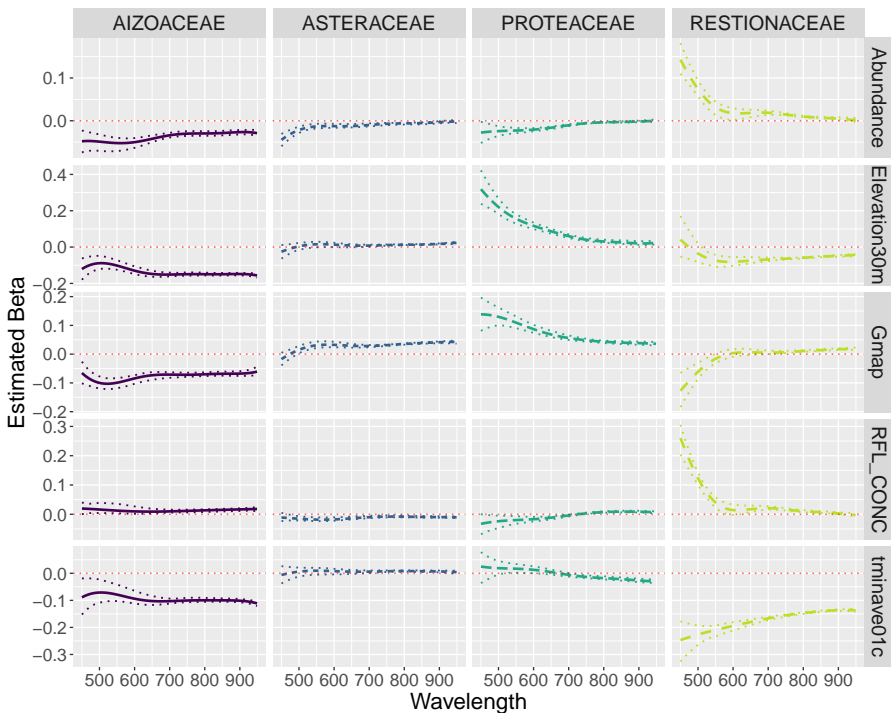


Fig. 6 Estimated regression coefficient functions $\beta^{(R)}(w)$ the reflectance spectrum for all families and environmental predictors.

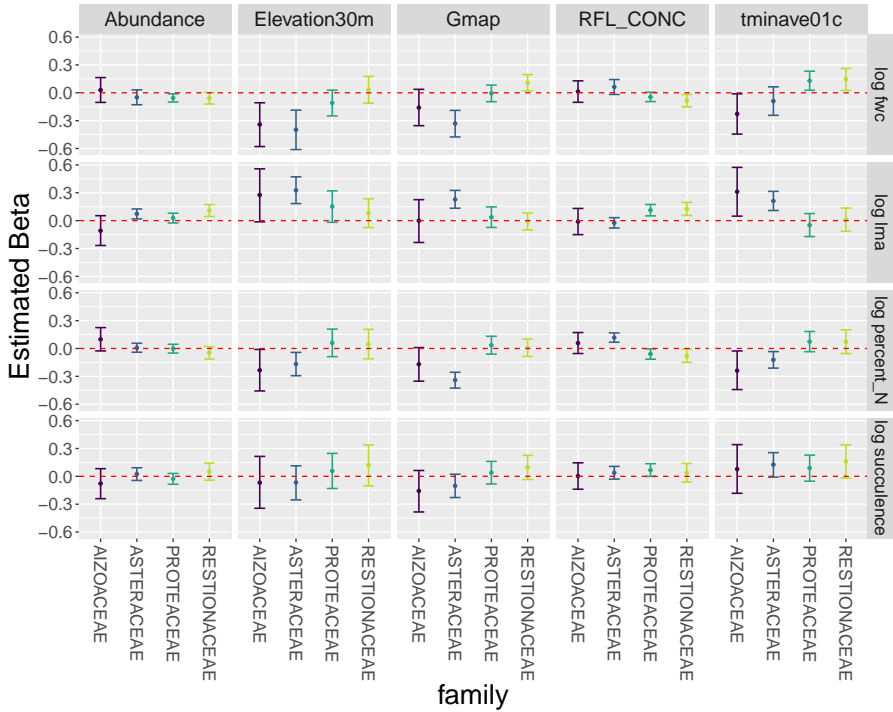


Fig. 7 Estimated regression coefficients $\beta^{(T)}$ for all traits, families, and environmental predictors.

4.2.1 Aizoaceae

For Aizoaceae, reflectances have a negative relationship with abundance, elevation, annual precipitation and temperature for all wavelengths. In contrast, Aizoaceae's reflectances have a very weak positive relationship with rainfall concentration. Although the relationships are generally weak, it is the only family whose entire reflectance spectrum is related to all covariates. We suspect that this could be a signal of overall leaf succulence given that precipitation and temperature have similar relationships and the expectation for leaves to be driven towards succulence as an adaptation to drier and hotter environments. Alternatively these family wide responses could be the result of other unmeasured traits such as those in leaf epidermal surfaces (Heim et al., 2015).

In terms of traits, elevation has a significant negative relationship with leaf water content (LWC) and percent nitrogen (pN). Temperature has a positive relationship with leaf mass per area (LMA) but negative relationships with LWC and pN. The LMA and temperature relationship roughly matches expectations found by the Leaf Economic Spectrum (LES), a study that examined trait and environment relationships at a global scale for a large sample of species (Wright et al., 2004). The LES also finds that nitrogen and leaf mass per area tend to be negatively related, fitting in with our results as well.

4.2.2 Asteraceae

For Asteraceae, the effects of all environmental covariates are very weak for the entire reflectance spectrum even though there are many significant estimated effects. Specifically, abundance and rainfall concentration are slightly negatively associated with log reflectance less than 700 nm, while annual precipitation has a weak positive relationship with reflectance for all wavelengths over 500 nm. Out of the families chosen, the Asteraceae appear to have some of the weakest environmental signals for reflectance. This may be attributable to the fact that the Asteraceae is one of the most widely distributed groups across the Greater Cape Floristic Region, with a high diversity of growth forms, e.g., annuals, succulents and geophytes, tolerating a high number of environmental conditions (Manning and Goldblatt, 2012; Manning, 2013). This diversity would likely result in a high variation of reflectance signals that could weaken relationships.

LWC is negatively associated with elevation and annual precipitation, holding other covariates constant, while LMA is positively associated with elevation, precipitation, temperature, and abundance. The latter results have mixed correspondence to previous global analyses, with global LMA having negative to insignificant relationships with precipitation (Wright et al., 2004). Percent nitrogen is negatively associated with elevation, annual precipitation, and January's minimum temperature, while it is positively associated with rainfall concentration. Leaf succulence has a weak positive relationship with temperature, while all other covariates have 90% credible intervals that include 0. This partially matches the expectation that leaves would become succulent in more arid areas.

4.2.3 Proteaceae

Of the four families, the log reflectance of Proteaceae has the strongest relationship with elevation and annual precipitation. For elevation, reflectance has a strong positive relationship for shorter wavelengths and a weak positive relationship for longer wavelengths. As iterated previously, we interpret the environment and reflectance relationships in Figure 6 as indicating trends in leaf traits that are unmeasured but varying across the environment. In the case of elevation and the visible region, this may be a trend in traits such as photosynthetic pigments which are strongly associated in the visible region of spectra (Jacquemoud and Ustin, 2019c). The estimated relationships between reflectance and annual precipitation is positive and significant for all wavelengths, likely representing changes in traits co-correlated with the amount of water in leaves. Reflectance has a weak negative relationship with temperature for wavelengths greater than 700 nm. Similarly, the relationship between abundance and reflectance is negative for wavelengths less than 750 nm.

In general, Proteaceae's traits have weak relationships with environmental covariates and abundance. However, LWC reveals a slightly positive relationship with temperature and negative relationship with abundance while LMA

has a slightly positive relationship with rainfall concentration. In a study of the genus *Protea*, a prominent genus of the Proteaceae family within the Greater Cape Floristic Region, [Mitchell et al. \(2015\)](#) found similar results for the LWC and temperature relationship (though theirs were non-significant) and LMA and rainfall seasonality (a related measure to rainfall concentration).

4.2.4 Restionaceae

Although Restionaceae showed very weak correlations between traits and reflectance, reflectance is strongly connected with environmental covariates for shorter wavelengths, suggesting a shift in underlying traits associated with the visible region, e.g., photosynthetic pigments, along environmental gradients. Abundance and rainfall concentration are positively related to reflectance at short wavelengths, while both annual precipitation and temperature are negatively related to reflectance. We estimate that increases in temperature are related to decreases in reflectance for all wavelengths. For wavelengths above 525 nm, we find a negative relationship between elevation and reflectance.

Turning to traits, Restionaceae's LWC is slightly positively related to temperature and annual precipitation but appears to be negatively related to abundance and rainfall concentration. Leaf mass area has slight positive relationships with rainfall concentration and abundance. For log pN and LS, all 90% credible intervals include 0. We suspect that the lack of clear trait and environmental trends could be a result of other known environmental drivers, e.g., fire and soil fertility, that drive differing adaptive strategies within the Restionaceae ([Wüest et al., 2016](#)).

5 Summary and Future Work

For four plant families within the Greater Cape Floristic Region, we have presented modeling to enable assessment of the importance of environmental/habitat predictors in predicting traits and reflectance. This approach allows us to address the novel question of how trait and reflectance vary along environmental gradients. For remote sensing efforts aimed at regional and global extents, this question should be of immediate interest since it is the shifting nature of these relationships across different sets of plant functional types that reduces the generalizability of empirical models for trait prediction ([Schimel et al., 2015](#); [Kothari and Schweiger, 2022](#); [Wang et al., 2022](#)). Our current model presents an initial step in exploring an area that we feel has been underutilized in ecology given a lack of available statistical tools. Lastly, we have shown that joint modeling of traits and reflectances provides better conditional predictive performance than modeling them independently.

In future work, our approaches could be adapted to include discrete or categorical traits, as in [Schliep and Hoeting \(2013\)](#) or [Clark et al. \(2017\)](#). Extending the framework in [White et al. \(2022\)](#) to spatially model the dependence between traits and reflectance would also be of interest, possibly including shape constraints [White et al. \(2021\)](#). In addition, with richer datasets, we

could explore how reflectance/trait relationships vary along environmental gradients. Overall, the functional data approach in ecology is underutilized despite a plethora of ecological data that would be suitable for such analysis, e.g., spectral reflectance, organismal movement, and time series. We envision models incorporating joint responses of both scalar and functional data will be of high value to ecological problems beyond those in the present study.

Acknowledgments. We thank Matthew Aiello-Lammens, Douglas Euston-Brown, Hayley Kilroy Mollmann, Cory Merow, Jasper Slingsby, Helga van der Merwe, and Adam Wilson for their contributions in the data collection and curation. Special thanks to Cape Nature and the Northern Cape Department of Environment and Nature Conservation for permission for the collection of leaf spectra and traits. Data collection efforts were made possible by funding from National Science Foundation grant DEB-1046328 to J.A. Silander. Additional support was provided by NASA with a Future Investigators in NASA Earth and Space Science and Technology (FINESST) grant award (80NSSC20K1659) to H.A. Frye and J.A. Silander.

Appendix A Markov Chain Monte Carlo Details

In this section, we provide the full conditional distributions used for the Gibb's sampler. We use $\theta|\cdots$ to denote the full conditional distribution of the parameter θ . For simplicity, we let \mathbf{T} be an $n \times s$ matrix of all observed traits and \mathbf{R} be an $n \times 500$ log reflectances. For traits and reflectances, respectively, we use $r_{-\theta}^{(T)}$ and $r_{-\theta}^{(R)}$ to be the residuals when excluding a the parameter θ (θ is used as a placeholder). For example, $r_{-\beta^{(R)}}^{(R)}$ is the residuals when removing the environmental regression from the model. In the case of wavelength-varying parameters, we use a similar notation to indicate the exclusion of the first term in a vector (e.g., θ_{-1}). In addition, we let D_σ be diagonal matrix with elements of $\sigma^2(w)$ and $D_{\beta^{(R)}}$ is a diagonal matrix with the prior variances given in (3). In the case of updates for \mathbf{U}_j , we refer to terms defined in Section 3.3. The posterior conditional distributions are as follows:

$$\begin{aligned}
 \text{vec}(\mathbf{B}^{(R)}) &\sim N(\Sigma_{\beta_R} \mu_{\beta_R}, \Sigma_{\beta_R}) & \mathbf{U}_j^{(R)} &\sim N(\Sigma_{U_j} \mu_{U_j}, \Sigma_{U_j}) \\
 \text{vec}(\mathbf{B}^{(T)}) &\sim N(\Sigma_{\beta_T} \mu_{\beta_T}, \Sigma_{\beta_T}) & \sigma_\alpha^{-2} &\sim \text{Gamma}(a_\alpha, b_\alpha) \\
 \boldsymbol{\alpha}^{*(R)} &\sim N(\Sigma_{\alpha_R} \mu_{\alpha_R}, \Sigma_{\alpha_R}) & \sigma_{\beta_k}^{-2} &\sim \text{Gamma}(a_{\beta_k}, b_{\beta_k}) \\
 \boldsymbol{\alpha}^{(T)} &\sim N(\Sigma_{\alpha_T} \mu_{\alpha_T}, \Sigma_{\alpha_T}) & \boldsymbol{\Omega}^{-1} &\sim \text{Wishart}(\nu_\Omega, S_\Omega)
 \end{aligned} \tag{A1}$$

$$\begin{aligned}
\mu_{\beta_R} &= (\mathbf{K}'_{\beta} \otimes \mathbf{E}') \text{vec} \left(r_{-\beta^{(R)}}^{(R)} D_{\sigma}^{-1} \right) \\
\Sigma_{\beta_R} &= \left(\mathbf{K}'_{\beta} D_{\sigma}^{-1} \mathbf{K}_{\beta} \otimes \mathbf{E}' \mathbf{E} + D_{\beta^{(R)}}^{-1} \right)^{-1} \\
\mu_{\beta_T} &= (\mathbb{I}_{s \times s} \otimes \mathbf{E}') \text{vec} \left(r_{-\beta^{(T)}}^{(T)} \Omega^{(T)-1} \right) \\
\Sigma_{\beta_T} &= \left(\Omega^{(T)-1} \otimes \mathbf{E}' \mathbf{E} + D_{\beta^{(T)}}^{-1} \right)^{-1} \\
\mu_{\alpha_R} &= \mathbf{K}'_{\alpha} \mathbf{1}' r_{-\alpha^{(R)}}^{(R)} D_{\sigma}^{-1} \\
\Sigma_{\alpha_R} &= \left(n \mathbf{K}'_{\alpha} D_{\sigma}^{-1} \mathbf{K}_{\alpha} + D_{\alpha^{(R)}}^{-1} \right)^{-1} \\
\mu_{\alpha_T} &= \mathbf{K}'_{\alpha} \mathbf{1}' r_{-\alpha^{(T)}}^{(R)} \Omega^{(T)-1} \\
\Sigma_{\alpha_T} &= \left(n \Omega^{(T)-1} + D_{\alpha^{(T)}}^{-1} \right)^{-1} \\
\mu_{U_j} &= \mathbf{K}'_U D_{\sigma}^{-1} r_j^{(R)} -_{U_j} + \Sigma_{R_j|T_j}^{-1} \mu_{R_j|T_j} \\
\Sigma_{U_j} &= \left(\mathbf{K}'_U D_{\sigma}^{-1} \mathbf{K}_U + \Sigma_{R_j|T_j}^{-1} \right)^{-1} \\
a_{\alpha} &= 1 + (N_{\alpha} - 1)/2 \\
b_{\alpha} &= 1 + (\boldsymbol{\alpha}_{-1}^{*(R)})' \boldsymbol{\alpha}_{-1}^{*(R)}/2 \\
a_{\beta_k} &= 1 + (N_{\beta} - 1)/2 \\
b_{\beta_k} &= 1 + (\mathbf{B}_{-1,k}^{(R)})' \mathbf{B}_{-1,k}^{(R)}/2 \\
\nu_{\Omega} &= N_U + s + 1 + n \\
S_{\Omega} &= (10^{-3} \mathbb{I} + \mathbf{U}' \mathbf{U})^{-1}
\end{aligned} \tag{A2}$$

Appendix B Model Comparison

In Tables B1 - B3, we present the cross-validation results (in order) for Restionaceae, Proteaceae, and Aizoaceae. The joint model improves out-of-sample prediction performance for reflectances for all families, and this benefit is significant. On the other hand, the conditional out-of-sample prediction performance for traits depends on the family. For Asteraceae and Restionaceae, the families with the most data, prediction of plant traits benefits from joint modeling of traits and reflectance. For Proteaceae, plant trait predictions are slightly better under the independent model using the ES. However, we emphasize that the improved prediction is minimal for the independent model. For Aizoaceae, the family with the fewest data, prediction of plant traits suffers under the joint model. In summary, we find that reflectance predictions are uniformly and significantly better under the joint model for all plant families. Trait predictions are better under the joint model for two of the four families (in terms of ES) and only marginally worse for Proteaceae. We speculate that the benefit of the joint model appears when there is enough data to adequately estimate the relationship between traits and reflectance. Based on these findings, we use the joint model to present interpretation of the results.

References

Aiello-Lammens, M. E., Slingsby, J. A., Merow, C., Mollmann, H. K., Euston-Brown, D., Jones, C. S., and Silander Jr, J. A. (2017). Processes of community assembly in an environmentally heterogeneous, high biodiversity region. *Ecography*, 40(4):561–576. Publisher: Wiley Online Library.

Table B1 Model comparison between joint and independent models for Restionaceae.

Quantity	Model	MAE	RMSE	ES
log lma	[T E][R E]	0.354	0.431	0.585
log fwc	[T E][R E]	0.297	0.384	
log succulence	[T E][R E]	0.443	0.580	
log percent_N	[T E][R E]	0.345	0.420	
log Reflectance	[T E][R E]	0.587	1.079	17.925
log lma	[T, R E]	0.294	0.424	0.488
log fwc	[T, R E]	0.239	0.315	
log succulence	[T, R E]	0.333	0.439	
log percent_N	[T, R E]	0.306	0.532	
log Reflectance	[T, R E]	0.162	0.260	3.900

Table B2 Model comparison between joint and independent models for Proteaceae.

Quantity	Model	MAE	RMSE	ES
log lma	[T E][R E]	0.246	0.322	0.397
log fwc	[T E][R E]	0.186	0.274	
log succulence	[T E][R E]	0.283	0.367	
log percent_N	[T E][R E]	0.217	0.287	
log Reflectance	[T E][R E]	0.449	0.773	13.107
log lma	[T, R E]	0.250	0.325	0.405
log fwc	[T, R E]	0.215	0.303	
log succulence	[T, R E]	0.279	0.361	
log percent_N	[T, R E]	0.238	0.303	
log Reflectance	[T, R E]	0.139	0.224	3.432

Table B3 Model comparison between joint and independent models for Aizoaceae.

Quantity	Model	MAE	RMSE	ES
log lma	[T E][R E]	0.496	0.322	0.728
log fwc	[T E][R E]	0.409	0.274	
log succulence	[T E][R E]	0.490	0.367	
log percent_N	[T E][R E]	0.394	0.287	
log Reflectance	[T E][R E]	0.444	0.773	12.705
log lma	[T, R E]	0.793	0.325	1.063
log fwc	[T, R E]	0.601	0.303	
log succulence	[T, R E]	0.445	0.361	
log percent_N	[T, R E]	0.621	0.303	
log Reflectance	[T, R E]	0.140	0.224	3.158

Anderegg, L. D. L., Berner, L. T., Badgley, G., Sethi, M. L., Law, B. E., and HilleRisLambers, J. (2018). Within-species patterns challenge our understanding of the leaf economics spectrum. *Ecology Letters*, 21(5):734–744.

Asner, G. P., Martin, R. E., Ford, A. J., Metcalfe, D. J., and Liddell, M. J. (2009). Leaf chemical and spectral diversity in Australian tropical forests. *Ecological Applications*, 19(1):236–253.

Asner, G. P., Martin, R. E., Tupayachi, R., Emerson, R., Martinez, P., Sinca, F., Powell, G. V. N., Wright, S. J., and Lugo, A. E. (2011). Taxonomy and remote sensing of leaf mass per area (LMA) in humid tropical forests. *Ecological Applications*, 21(1):85–98.

- Born, J., Linder, H. P., and Desmet, P. (2006). The Greater Cape Floristic Region: Greater Cape Floristic Region. *Journal of Biogeography*, 34(1):147–162.
- Cadotte, M. W., Carscadden, K., and Mirotchnick, N. (2011). Beyond species: functional diversity and the maintenance of ecological processes and services: Functional diversity in ecology and conservation. *Journal of Applied Ecology*, 48(5):1079–1087.
- Caturegli, L., Matteoli, S., Gaetani, M., Grossi, N., Magni, S., Minelli, A., Corsini, G., Remorini, D., and Volterrani, M. (2020). Effects of water stress on spectral reflectance of bermudagrass. *Scientific Reports*, 10(1):15055.
- Cavender-Bares, J., Schneider, F. D., Santos, M. J., Armstrong, A., Carnaval, A., Dahlin, K. M., Fatoyinbo, L., Hurtt, G. C., Schimel, D., Townsend, P. A., Ustin, S. L., Wang, Z., and Wilson, A. M. (2022). Integrating remote sensing with ecology and evolution to advance biodiversity conservation. *Nature Ecology & Evolution*, 6(5):506–519.
- Clark, J. S., Nemerut, D., Seyednasrollah, B., Turner, P. J., and Zhang, S. (2017). Generalized joint attribute modeling for biodiversity analysis: Median-zero, multivariate, multifarious data. *Ecological Monographs*, 87(1):34–56.
- Coops, N., Dury, S., Smith, M.-L., Martin, M., and Ollinger, S. (2002). Comparison of green leaf eucalypt spectra using spectral decomposition. *Australian Journal of Botany*, 50(5):567.
- Díaz, S. and Cabido, M. (2001). Vive la différence: plant functional diversity matters to ecosystem processes. *Trends in Ecology & Evolution*, 16(11):646–655.
- Frye, H. A., Aiello-Lammens, M. E., Euston-Brown, D., Jones, C. S., Kilroy Mollmann, H., Merow, C., Slingsby, J. A., Merwe, H., Wilson, A. M., and Silander, J. A. (2021). Plant spectral diversity as a surrogate for species, functional and phylogenetic diversity across a hyper-diverse biogeographic region. *Global Ecology and Biogeography*, 30(7):1403–1417.
- Gneiting, T. and Raftery, A. E. (2007). Strictly proper scoring rules, prediction, and estimation. *Journal of the American Statistical Association*, 102(477):359–378.
- Heim, R., Jürgens, N., Große-Stoltenberg, A., and Oldeland, J. (2015). The Effect of Epidermal Structures on Leaf Spectral Signatures of Ice Plants (Aizoaceae). *Remote Sensing*, 7(12):16901–16914.
- Higdon, D. (2002). Space and space-time modeling using process convolutions. In *Quantitative Methods for Current Environmental Issues*, pages 37–56. Springer.
- Hmimina, G., Dufrière, E., and Soudani, K. (2014). Relationship between photochemical reflectance index and leaf ecophysiological and biochemical parameters under two different water statuses: towards a rapid and efficient correction method using real-time measurements: Disentangling PRI variability. *Plant, Cell & Environment*, 37(2):473–487.

- Inoue, Y. and Peñuelas, J. (2006). Relationship between light use efficiency and photochemical reflectance index in soybean leaves as affected by soil water content. *International Journal of Remote Sensing*, 27(22):5109–5114.
- Jacquemoud, S. and Ustin, S. (2019a). *Leaf Optical Properties*. Cambridge University Press, 1 edition.
- Jacquemoud, S. and Ustin, S. (2019b). *Leaf optical properties*. Cambridge University Press.
- Jacquemoud, S. and Ustin, S. (2019c). Variation Due to Leaf structural, Chemical, and Physiological Traits. In *Leaf Optical Properties*. Cambridge University Press, 1 edition.
- Jacquemoud, S. and Ustin, S. (2019d). Variations Due to Leaf Abiotic and Biotic Factors. In *Leaf Optical Properties*. Cambridge University Press, 1 edition.
- Jetz, W., Cavender-Bares, J., Pavlick, R., Schimel, D., Davis, F. W., Asner, G. P., Guralnick, R., Kattge, J., Latimer, A. M., Moorcroft, P., Schaepman, M. E., Schildhauer, M. P., Schneider, F. D., Schrodt, F., Stahl, U., and Ustin, S. L. (2016). Monitoring plant functional diversity from space. *Nature Plants*, 2(3):16024.
- JPL, N. (2020). NASADEM Merged DEM Global 1 arc second V001. Type: dataset.
- Kothari, S. and Schweiger, A. K. (2022). Plant spectra as integrative measures of plant phenotypes. *Journal of Ecology*, pages 1365–2745.13972.
- Latimer, A. M., Silander, J. A., and Cowling, R. M. (2005). Neutral Ecological Theory Reveals Isolation and Rapid Speciation in a Biodiversity Hot Spot. *Science*, 309(5741):1722–1725.
- Laughlin, D. C., Lusk, C. H., Bellingham, P. J., Burslem, D. F. R. P., Simpson, A. H., and Kramer-Walter, K. R. (2017). Intraspecific trait variation can weaken interspecific trait correlations when assessing the whole-plant economic spectrum. *Ecology and Evolution*, 7(21):8936–8949.
- Manning, J. (2013). *The Extra Cape flora*. Number 2 in Plants of the Greater Cape floristic region / John Manning and Peter Goldblatt. SANBI, Pretoria.
- Manning, J. and Goldblatt, P., editors (2012). *Plants of the Greater Cape Floristic Region*. Number 29 in Strelitzia. SANBI, Biodiversity for Life, Pretoria.
- McGill, B., Enquist, B., Weiher, E., and Westoby, M. (2006). Rebuilding community ecology from functional traits. *Trends in Ecology & Evolution*, 21(4):178–185.
- Meireles, J. E., Cavender-Bares, J., Townsend, P. A., Ustin, S., Gamon, J. A., Schweiger, A. K., Schaepman, M. E., Asner, G. P., Martin, R. E., Singh, A., Schrodt, F., Chlus, A., and O’Meara, B. C. (2020). Leaf reflectance spectra capture the evolutionary history of seed plants. *New Phytologist*, 228(2):485–493.
- Mitchell, N., Lewis, P. O., Lemmon, E. M., Lemmon, A. R., and Holsinger, K. E. (2017). Anchored phylogenomics improves the resolution of evolutionary relationships in the rapid radiation of *Protea* L. *American Journal of*

- Botany*, 104(1):102–115.
- Mitchell, N., Moore, T. E., Mollmann, H. K., Carlson, J. E., Mocko, K., Martinez-Cabrera, H., Adams, C., Silander, J. A., Jones, C. S., Schlichting, C. D., and Holsinger, K. E. (2015). Functional Traits in Parallel Evolutionary Radiations and Trait-Environment Associations in the Cape Floristic Region of South Africa. *The American Naturalist*, 185(4):525–537.
- Myers, N., Mittermeier, R. A., Mittermeier, C. G., Da Fonseca, G. A., and Kent, J. (2000). Biodiversity hotspots for conservation priorities. *Nature*, 403(6772):853–858.
- O’Connor, M. I., Gonzalez, A., Byrnes, J. E. K., Cardinale, B. J., Duffy, J. E., Gamfeldt, L., Griffin, J. N., Hooper, D., Hungate, B. A., Paquette, A., Thompson, P. L., Dee, L. E., and Dolan, K. L. (2017). A general biodiversity-function relationship is mediated by trophic level. *Oikos*, 126(1):18–31.
- Orcival, J. M., Joffre, R., and Rambal, S. (1999). Exploring the relationships between reflectance and anatomical and biochemical properties in *Quercus ilex* leaves. *New Phytologist*, 143(2):351–364.
- Pau, S., Nippert, J. B., Slapikas, R., Griffith, D., Bachle, S., Helliker, B. R., O’Connor, R. C., Riley, W. J., Still, C. J., and Zaricor, M. (2022). Poor relationships between NEON Airborne Observation Platform data and field-based vegetation traits at a mesic grassland. *Ecology*, 103(2).
- Penuelas, J., Pinol, J., Ogaya, R., and Filella, I. (1997). Estimation of plant water concentration by the reflectance Water Index WI (R900/R970). *International Journal of Remote Sensing*, 18(13):2869–2875.
- Peñuelas, J., Filella, I., Biel, C., Serrano, L., and Savé, R. (1993). The reflectance at the 950–970 nm region as an indicator of plant water status. *International Journal of Remote Sensing*, 14(10):1887–1905.
- Pirie, M. D., Oliver, E. G. H., Mugrabi de Kuppler, A., Gehrke, B., Le Maitre, N. C., Kandziora, M., and Bellstedt, D. U. (2016). The biodiversity hotspot as evolutionary hot-bed: spectacular radiation of Erica in the Cape Floristic Region. *BMC Evolutionary Biology*, 16(1):190.
- Pu, R., Ge, S., Kelly, N. M., and Gong, P. (2003). Spectral absorption features as indicators of water status in coast live oak (*Quercus agrifolia*) leaves. *International Journal of Remote Sensing*, 24(9):1799–1810.
- Ramsay, J. (2005). Functional data analysis. *Encyclopedia of Statistics in Behavioral Science*.
- Ramsay, J. O. and Silverman, B. W. (2007). *Applied functional data analysis: Methods and case studies*. Springer.
- Reich, P. B., Ellsworth, D. S., Walters, M. B., Vose, J. M., Gresham, C., Volin, J. C., and Bowman, W. D. (1999). Generality of Leaf Trait Relationships: A test across six biomes. *Ecology*, 80(6):1955–1969.
- Reich, P. B., Walters, M. B., and Ellsworth, D. S. (1997). From tropics to tundra: Global convergence in plant functioning. *Proceedings of the National Academy of Sciences*, 94(25):13730–13734.

- Ripullone, F., Rivelli, A. R., Baraldi, R., Guarini, R., Guerrieri, R., Magnani, F., Peñuelas, J., Raddi, S., and Borghetti, M. (2011). Effectiveness of the photochemical reflectance index to track photosynthetic activity over a range of forest tree species and plant water statuses. *Functional Plant Biology*, 38(3):177.
- Rodríguez-Pérez, J. R., Riaño, D., Carlisle, E., Ustin, S., and Smart, D. R. (2007). Evaluation of Hyperspectral Reflectance Indexes to Detect Grapevine Water Status in Vineyards. *American Journal of Enology and Viticulture*, 58(3). Publisher: American Journal of Enology and Viticulture Section: Article.
- Schimel, D., Pavlick, R., Fisher, J. B., Asner, G. P., Saatchi, S., Townsend, P., Miller, C., Frankenberg, C., Hibbard, K., and Cox, P. (2015). Observing terrestrial ecosystems and the carbon cycle from space. *Global Change Biology*, 21(5):1762–1776.
- Schleuning, M., Neuschulz, E. L., Albrecht, J., Bender, I. M., Bowler, D. E., Dehling, D. M., Fritz, S. A., Hof, C., Mueller, T., Nowak, L., Sorensen, M. C., Böhning-Gaese, K., and Kissling, W. D. (2020). Trait-Based Assessments of Climate-Change Impacts on Interacting Species. *Trends in Ecology & Evolution*, 35(4):319–328.
- Schliep, E. M., Gelfand, A. E., Mitchell, R. M., Aiello-Lammens, M. E., and Silander Jr, J. A. (2018). Assessing the joint behaviour of species traits as filtered by environment. *Methods in Ecology and Evolution*, 9(3):716–727.
- Schliep, E. M. and Hoeting, J. A. (2013). Multilevel latent gaussian process model for mixed discrete and continuous multivariate response data. *Journal of Agricultural, Biological, and Environmental Statistics*, 18(4):492–513.
- Schulze, R. E. (1997). South African atlas of agrohydrology and climatology: Contribution towards a final report to the water research commission on project 492. Technical Report TT82-96, Water Resource Commission, Pretoria, South Africa.
- Schweiger, A. K., Cavender-Bares, J., Townsend, P. A., Hobbie, S. E., Madritch, M. D., Wang, R., Tilman, D., and Gamon, J. A. (2018). Plant spectral diversity integrates functional and phylogenetic components of biodiversity and predicts ecosystem function. *Nature Ecology & Evolution*, 2(6):976–982.
- Seelig, H., Hoehn, A., Stodieck, L. S., Klaus, D. M., Adams III, W. W., and Emery, W. J. (2008). The assessment of leaf water content using leaf reflectance ratios in the visible, near-, and short-wave-infrared. *International Journal of Remote Sensing*, 29(13):3701–3713.
- Serbin, S. P., Wu, J., Ely, K. S., Kruger, E. L., Townsend, P. A., Meng, R., Wolfe, B. T., Chlus, A., Wang, Z., and Rogers, A. (2019). From the Arctic to the tropics: multibiome prediction of leaf mass per area using leaf reflectance. *New Phytologist*, 224(4):1557–1568.
- Shiklomanov, A. N., Dietze, M. C., Viskari, T., Townsend, P. A., and Serbin, S. P. (2016). Quantifying the influences of spectral resolution on uncertainty in leaf trait estimates through a Bayesian approach to RTM inversion.

- Remote Sensing of Environment*, 183:226–238.
- Singh, A., Serbin, S. P., McNeil, B. E., Kingdon, C. C., and Townsend, P. A. (2015). Imaging spectroscopy algorithms for mapping canopy foliar chemical and morphological traits and their uncertainties. *Ecological Applications*, 25(8):2180–2197.
- Thenot, F., Méthy, M., and Winkel, T. (2002). The Photochemical Reflectance Index (PRI) as a water-stress index. *International Journal of Remote Sensing*, 23(23):5135–5139.
- Turner, W. (2014). Sensing biodiversity. *Science*, 346(6207):301–302.
- Verboom, G. A., Archibald, J. K., Bakker, F. T., Bellstedt, D. U., Conrad, F., Dreyer, L. L., Forest, F., Galley, C., Goldblatt, P., Henning, J. F., Mummehoff, K., Linder, H. P., Muasya, A. M., Oberlander, K. C., Savolainen, V., Snijman, D. A., Niet, T. v. d., and Nowell, T. L. (2009). Origin and diversification of the Greater Cape flora: Ancient species repository, hot-bed of recent radiation, or both? *Molecular Phylogenetics and Evolution*, 51(1):44–53.
- Wang, Z., Townsend, P. A., and Kruger, E. L. (2022). Leaf spectroscopy reveals divergent inter- and intra-species foliar trait covariation and trait–environment relationships across NEON domains. *New Phytologist*, 235(3):923–938.
- Wüest, R. O., Litsios, G., Forest, F., Lexer, C., Linder, H. P., Salamin, N., Zimmermann, N. E., and Pearman, P. B. (2016). Resprouter fraction in Cape Restionaceae assemblages varies with climate and soil type. *Functional Ecology*, 30(9):1583–1592.
- White, P. A., Frye, H., Christensen, M. F., Gelfand, A. E., and Silander Jr, J. A. (2022). Spatial functional data modeling of plant reflectances. *Annals of Applied Statistics*.
- White, P. A., Keeler, D. G., and Rupper, S. (2021). Hierarchical integrated spatial process modeling of monotone west antarctic snow density curves. *The Annals of Applied Statistics*, 15(2):556–571.
- Wright, I. J., Reich, P. B., Westoby, M., Ackerly, D. D., Baruch, Z., Bongers, F., Cavender-Bares, J., Chapin, T., Cornelissen, J. H., Diemer, M., and others (2004). The worldwide leaf economics spectrum. *Nature*, 428(6985):821–827.
- Wright, J. P. and Sutton-Grier, A. (2012). Does the leaf economic spectrum hold within local species pools across varying environmental conditions? *Functional Ecology*, 26(6):1390–1398.
- Yang, X., Tang, J., Mustard, J. F., Wu, J., Zhao, K., Serbin, S., and Lee, J.-E. (2016). Seasonal variability of multiple leaf traits captured by leaf spectroscopy at two temperate deciduous forests. *Remote Sensing of Environment*, 179:1–12.
- Zhang, H. (2004). Inconsistent estimation and asymptotically equal interpolations in model-based geostatistics. *Journal of the American Statistical Association*, 99(465):250–261.